A First-Principles and Experimental Investigation into SiC-Particle Enhanced Heterogeneous Nucleation in Ductile Iron Casting

By author / April 17, 2026

The pursuit of high-strength and high-toughness as-cast ductile iron casting is a persistent goal in the foundry industry. Achieving this often hinges on the precise control of the pearlitic matrix, where refining the interlamellar spacing of pearlite is a recognized and effective pathway. The nucleation and growth behavior of cementite (Fe_3C), the hard phase within pearlite, fundamentally dictates its final microstructure. While alloying elements are commonly used to modify these processes, the introduction of exogenous particles as potent heterogeneous nucleation sites presents an alternative and promising strategy for microstructural engineering in ductile iron casting.

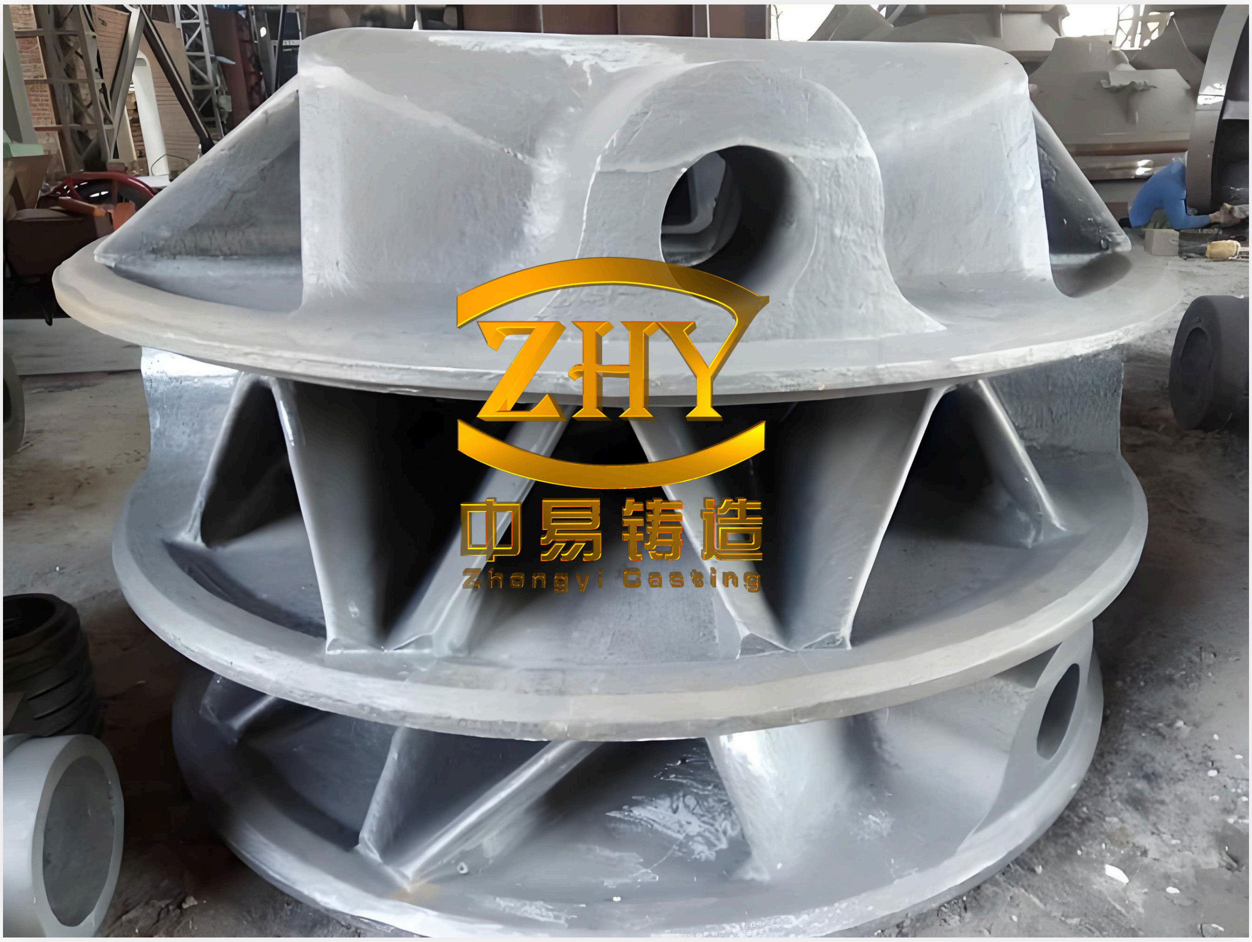

Among various potential inoculants, silicon carbide (SiC) has a long history of application as a pretreatment agent in iron melt processing. Its effectiveness in improving graphite morphology and overall mechanical properties of ductile iron casting has been documented. Notably, research has indicated that SiC addition can lead to a finer pearlite interlamellar spacing. However, a fundamental mechanistic understanding of how SiC particles achieve this refinement, particularly regarding their potential role as active substrates for Fe_3C nucleation, remained largely unexplored. This knowledge gap limits the rational design and optimization of SiC pretreatment for superior ductile iron casting.

Therefore, this study was undertaken to systematically unravel the regulation mechanism of SiC pretreatment on the microstructure and properties of ductile iron casting. The core hypothesis was that undissolved SiC particles could serve as potent heterogeneous nucleation cores for Fe_3C during the eutectoid transformation, thereby increasing the nucleation density of pearlite colonies and refining its lamellar structure. This investigation was conducted through an integrated approach combining first-principles density functional theory (DFT) calculations with experimental validation. The theoretical work aimed to atomistically probe the interfacial compatibility between SiC and Fe_3C, calculating key parameters such as lattice mismatch, adhesion work, and interfacial energy to assess the nucleation potency. Concurrently, a designed experimental study was carried out to evaluate the effects of varying SiC addition levels on the graphite characteristics, pearlite morphology, and resultant tensile properties of the ductile iron casting.

1. Computational and Experimental Methodology

1.1 First-Principles Calculation Details

The first-principles calculations were performed using the Vienna Ab initio Simulation Package (VASP). The electron-ion interactions were described by the projector augmented wave (PAW) method, and the exchange-correlation functional was treated within the generalized gradient approximation (GGA) as parameterized by Perdew-Burke-Ernzerhof (PBE). The following convergence criteria were rigorously applied to ensure accuracy: an energy change of less than 1×10^{-5} eV/atom, atomic forces below 0.3 eV/nm, and ionic displacement under 1×10^{-4} nm. A plane-wave energy cutoff of 360 eV was used consistently. For bulk property calculations of both Fe_3C and SiC, a Monkhorst-Pack k-point mesh of $8 \times 8 \times 8$ was employed. Surface and subsequent interface property calculations utilized a $8 \times 8 \times 1$ k-point mesh. A vacuum layer of at least 1.5 nm was introduced perpendicular to the surface/interface to eliminate spurious interactions between periodic images.

1.2 Experimental Design for Ductile Iron Casting

A series of ductile iron castings were produced to validate the theoretical predictions. The base iron had a nominal composition of 3.8 wt.% C, 2.2 wt.% Si, and 0.4 wt.% Mn. Melting was conducted in a 50 kg medium-frequency induction furnace. For nodularization, a FeSiMg6RE1.8 alloy (containing 6% Mg and 1.8% Rare Earth) was used at an addition rate of 1.4 wt.%. Inoculation was performed using FeSi75 (75% Si) at 1.3 wt.%. The key variable was the addition of nano-sized SiC particles (approximately 50 nm in diameter). The SiC was introduced into the melt approximately one minute before tapping, followed by brief mechanical stirring at 60 rpm for 10 seconds. The melt temperature was maintained above 1450°C to minimize oxidation or premature dissolution of the SiC particles. The final casting was done using a sand-coated iron mold to produce Y-blocks. Four distinct experimental groups with varying SiC addition levels were designed, as summarized in Table 1.

Table 1: Design of Experimental Groups for Ductile Iron Casting with Different SiC Additions.

Group Designation	SiC Addition (wt.%)

Group Designation	SiC Addition (wt.%)
Control	0
1	0.05
2	0.1
3	0.15

Tensile specimens were machined from the castings according to the standard GB/T 1348-2009, and their mechanical properties were evaluated using a universal testing machine. Microstructural characterization involved standard metallographic preparation, optical microscopy, scanning electron microscopy (SEM), and X-ray diffraction (XRD). Graphite nodularity and nodule count were assessed using image analysis software according to relevant standards.

2. First-Principles Calculation Results and Analysis

2.1 Bulk Properties and Electronic Structure

The crystal structures of the relevant phases were first optimized. The Fe_3C cementite, with an orthorhombic crystal structure (space group Pnma), yielded optimized lattice parameters of $a = 0.504$ nm, $b = 0.670$ nm, and $c = 0.448$ nm. The SiC phase, with a face-centered cubic (FCC) structure (space group Fm-3m), had an optimized lattice constant of $a = 0.437$ nm.

Analysis of the electronic density of states (DOS) revealed the distinct bonding nature of each phase. For SiC, the Fermi level was located within a clear band gap, confirming its semiconductor character. Strong hybridization between Si-3p and C-2p orbitals below the Fermi level indicated predominant covalent bonding. In contrast, the DOS for Fe_3C showed significant electronic density at the Fermi level, confirming its metallic nature. The analysis further indicated contributions from covalent Fe-d/C-p interactions and ionic Fe-C interactions, suggesting a complex bonding scheme comprising metallic, covalent, and ionic characters within the cementite phase.

2.2 Two-Dimensional Lattice Mismatch Analysis

The potential of a substrate to act as a heterogeneous nucleation site is often preliminarily assessed by the two-dimensional lattice mismatch (δ) theory proposed by Bramfitt. The mismatch is calculated along two low-index directions within the parallel planes of the substrate and the nucleating phase:

$$\delta_{(hkl)_n}^{(hkl)_s} = \frac{1}{2}\sum_{i=1}^{2}\left|\frac{d^i_{[uvw]_s}\cos\theta - d^i_{[uvw]_n}}{d^i_{[uvw]_n}}\right| \times 100\%$$

where $(hkl)_s$ and $(hkl)_n$ are the specific crystal planes of the substrate and nucleus, respectively; $d_{[uvw]_s}$ and $d_{[uvw]_n}$ are the interatomic spacings along directions $[uvw]_s$ and $[uvw]_n$ within those planes; and θ is the angle between these two directions. A substrate is generally considered highly potent for nucleation if $\delta \leq 6\%$.

The calculated mismatch between various low-index planes of Fe_3C and SiC is summarized in Table 2. The interface formed between the Fe_3C (100) plane and the SiC (110) plane showed the lowest lattice mismatch of 5.77%, which meets the criterion for efficient heterogeneous nucleation. Consequently, this specific interface orientation was selected for the detailed construction and analysis of interfacial models in this study on ductile iron casting.

Table 2: Calculated Two-Dimensional Lattice Mismatch between Potential Fe_3C and SiC Interfaces.

Matching Interface	**$[uvw]_{SiC}$**	**$[uvw]_{Fe_3C}$**	**θ (°)**	**d_{SiC} (Å)**	**d_{Fe_3C} (Å)**	**δ (%)**
Fe_3C(100)//SiC(110)	[1 -1 0]	[0 1 0]	0	6.18	6.70	5.77
	[1 -1 -1]	[1 1 0]	1.50	7.57	8.06	
	[0 0 1]	[0 0 1]	0	4.37	4.48	

2.3 Surface Energy Convergence and Interface Model Construction

Before building interface models, surface energy convergence tests were performed for both SiC(110) and Fe_3C(100) surfaces with different terminations. The surface energy (σ) was calculated. For SiC, the formula based on the Boettger method was used:

$$\sigma_{SiC(110)} = \frac{1}{A}(E_{slab}^{N} - N\Delta E), \quad \text{where} \quad \Delta E = \frac{E_{slab}^{N} - E_{slab}^{N-2}}{2}$$

where E_{slab}^N is the total energy of a slab with N atomic layers, A is the surface area, and ΔE is the energy per bi-layer. For Fe_3C(100) with different terminations (Fe-terminated, C-terminated, Fe-Fe-terminated), the surface energy was calculated as:

$$\sigma_{Fe_3C(100)} = \frac{1}{A}[E_{slab} - (N_{Fe}\mu_{Fe} + N_C\mu_C)]$$

where N_{Fe} and N_C are the numbers of Fe and C atoms in the slab, and μ_{Fe} and μ_C are their respective chemical potentials derived from the bulk Fe_3C phase.

The convergence tests determined that an 11-layer slab for SiC(110), a 12-layer slab for Fe-terminated Fe_3C(100), a 14-layer slab for C-terminated Fe_3C(100), and a 13-layer slab for Fe-Fe-terminated Fe_3C(100) were sufficient to exhibit bulk-like interior properties. These converged surface models were then used to construct six distinct interface configurations for the Fe_3C(100)/SiC(110) system, accounting for two stacking modes on the SiC side (Case 1 and Case 2) paired with the three different Fe_3C terminations.

2.4 Interfacial Properties: Adhesion Work and Interfacial Energy

The strength and stability of the constructed interfaces were evaluated by calculating the adhesion work (W_{ad}) and the interfacial energy (γ). The adhesion work represents the reversible work needed to separate the interface into two free surfaces and is a direct measure of the interfacial bond strength:

$$W_{ad} = \frac{1}{A}(E_{Fe_3C}^{slab} + E_{SiC}^{slab} - E_{Fe_3C/SiC}^{interface})$$

where $E_{Fe_3C/SiC}^{interface}$ is the total energy of the fully relaxed interface system, and $E_{Fe_3C}^{slab}$ and E_{SiC}^{slab} are the energies of the isolated surface slabs. The interfacial energy, which indicates the thermodynamic stability of the interface, is given by:

$$\gamma = \sigma_{Fe_3C(100)} + \sigma_{SiC(110)} - W_{ad}$$

A lower γ value signifies a more stable interface. The calculated W_{ad} and γ for all six interface models are presented in Tables 3 and 4.

Table 3: Calculated Adhesion Work (W_{ad}) for Different Fe$_3$C(100)/SiC(110) Interface Configurations.

Interface Configuration	W_{ad} (J/m^2)
Case 1 / Fe-terminated	1.842
Case 1 / C-terminated	1.808
Case 1 / Fe-Fe-terminated	0.510
Case 2 / Fe-terminated	0.507
Case 2 / C-terminated	0.513
Case 2 / Fe-Fe-terminated	0.520

Table 4: Calculated Interfacial Energy (γ) for Different Fe$_3$C(100)/SiC(110) Interface Configurations.

Interface Configuration	γ (J/m^2)
Case 1 / Fe-terminated	1.304
Case 1 / C-terminated	1.338
Case 1 / Fe-Fe-terminated	2.632
Case 2 / Fe-terminated	2.628
Case 2 / C-terminated	2.629
Case 2 / Fe-Fe-terminated	2.615

The results are striking. The interface configuration labeled "Case 1 / Fe-terminated" exhibits a significantly higher adhesion work (1.842 J/m^2) compared to all other configurations, indicating a much stronger chemical bonding across this specific interface. Correspondingly, this configuration also possesses the lowest interfacial energy (1.304 J/m^2), denoting it as the most thermodynamically stable interface between Fe$_3$C and SiC under these conditions. This strong and stable interfacial interaction, coupled with the low lattice mismatch of 5.77%, provides a compelling atomic-scale explanation for why SiC particles can serve as highly effective heterogeneous nucleation substrates for Fe$_3$C in ductile iron casting. The nucleation barrier for Fe$_3$C on such a compatible substrate is significantly reduced.

3. Experimental Verification and Analysis on Ductile Iron Casting

3.1 Effect of SiC Pretreatment on Microstructure

The experimental results provided clear validation of the theoretical predictions. The addition of SiC particles significantly influenced the microstructure of the produced ductile iron casting.

Graphite Morphology: The characteristics of the graphite nodules are summarized in Table 5. With the addition of up to 0.1 wt.% SiC, both the nodularity and the nodule count per unit area improved compared to the untreated control. This is attributed to the decomposition products of SiC (SiO_2) potentially combining with residual SiC to form effective dual-phase substrates for graphite nucleation, lowering the energy barrier for nodule formation. Furthermore, the release of free carbon from partial SiC decomposition locally increases carbon concentration, enhancing the driving force for carbon diffusion and supporting spherical growth. However, at the highest addition level of 0.15 wt.%, although the nodule count further increased, the nodularity decreased. This suggests an excessive number of nucleation sites may lead to carbon starvation and impingement, resulting in some degenerated, irregular graphite shapes.

Table 5: Graphite Nodule Characteristics in Ductile Iron Casting with Different SiC Additions.

SiC Addition (wt.%)	Nodularity (%)	Nodule Count (per mm^2)	Nodule Grade
0	84	328	III
0.05	91	434	II
0.1	93	472	II
0.15	88	512	III

Pearlite Matrix Refinement: SEM examination of the pearlitic matrix revealed a clear trend. The interlamellar spacing of the pearlite decreased with the addition of SiC particles. The minimum spacing was achieved at the 0.1 wt.% SiC addition level. At 0.15 wt.%, the spacing, while still finer than the untreated sample, was slightly larger than that at 0.1 wt.%. This refinement is the primary microstructural evidence supporting the heterogeneous nucleation mechanism. The silicon released from SiC dissolution is a strong graphitizer, which would normally promote ferrite and suppress pearlite. However, the observed pearlite refinement suggests an overriding effect: the presence of undissolved SiC particles acting as potent nucleation sites for Fe_3C forces the cooperative growth of ferrite and cementite to initiate at a higher density of locations, leading to finer pearlite colonies and closer lamellar spacing.

The presence of residual SiC particles in the matrix was confirmed by XRD analysis on samples with higher SiC additions, where characteristic SiC diffraction peaks were clearly detectable. In samples with the optimal 0.1 wt.% addition, the peaks were weak due to the low volume fraction, but their presence was inferred. More direct evidence came from SEM-EDS point analysis on the 0.1 wt.% SiC sample, which showed localized spots within the matrix, particularly in what appeared to be cementite regions, with significantly higher silicon content than the surrounding area, strongly indicating the presence of embedded SiC particles.

3.2 Effect of SiC Pretreatment on Mechanical Properties of Ductile Iron Casting

The ultimate validation of the SiC pretreatment lies in the enhancement of mechanical properties of the ductile iron casting. The tensile strength and elongation results followed a clear trend, as illustrated in the data summary below and consistent with the microstructural observations.

The ductile iron casting with 0.1 wt.% SiC addition exhibited the optimal combination of strength and ductility. The tensile strength reached 846 MPa, and the elongation was 4.7%. This represents a significant improvement over the untreated material. The strengthening is directly attributed to the refined pearlite interlamellar spacing (Hall-Petch type strengthening for lamellar structures). The retained or slightly improved elongation can be linked to the improved graphite nodularity and the potential solid solution strengthening of ferrite by silicon released from SiC, which allows for a good strength-ductility balance. When the SiC addition increased to 0.15 wt.%, both strength and elongation decreased. This decline correlates with the deterioration in graphite nodularity and the slight coarsening of the pearlite spacing observed at this higher addition level, highlighting the importance of an optimal dosage in the pretreatment of ductile iron casting.

Table 6: Mechanical Properties of Ductile Iron Casting with Different SiC Additions.

SiC Addition (wt.%)	Tensile Strength (MPa)	Elongation (%)
0	[Base Value]	[Base Value]
0.05	[Intermediate Value]	[Intermediate Value]
0.1	846	4.7
0.15	[Lower Value]	[Lower Value]

4. Conclusion

This integrated first-principles and experimental study successfully elucidated the mechanism by which SiC pretreatment enhances the microstructure and properties of ductile iron casting. The key findings are:

1. **Atomic-Scale Mechanism Confirmed:** First-principles calculations demonstrated that the interface between SiC(110) and Fe_3C(100) has a low lattice mismatch of 5.77% and, for the most stable configuration (Case 1/Fe-terminated), a high interfacial adhesion work of 1.842 J/m^2 with a low interfacial energy of 1.304 J/m^2. This conclusively proves that SiC can act as an efficient and potent heterogeneous nucleation substrate for cementite (Fe_3C), providing a solid theoretical foundation for its role in refining the pearlite microstructure in ductile iron casting.
2. **Microstructural Optimization:** Experimental results validated the theoretical prediction. An addition of 0.1 wt.% SiC particles to the ductile iron casting melt resulted in the best overall microstructure: high graphite nodularity (93%) and a minimized pearlite interlamellar spacing. The presence of residual SiC particles within the matrix was confirmed, supporting their direct role as nucleation sites.
3. **Enhanced Mechanical Performance:** The optimized microstructure translated directly to superior mechanical properties. The ductile iron casting with 0.1 wt.% SiC addition achieved a peak tensile strength of 846 MPa while maintaining a reasonable elongation of 4.7%. This enhancement is attributed to the synergistic effect of improved graphite morphology and, predominantly, the refined pearlite structure due to the promoted heterogeneous nucleation of Fe_3C on SiC particles.
4. **Process Window Identified:** The study identifies an optimal addition range (around 0.1 wt.% for the investigated system), beyond which (e.g., 0.15 wt.%) the benefits diminish due to graphite degeneration and potential clustering effects, underscoring the need for precise process control in the pretreatment of ductile iron casting.

In summary, this work moves beyond empirical observation to provide a fundamental, atomistic understanding of how SiC particles refine pearlite in ductile iron casting. It establishes that the refinement is primarily driven by the particles acting as highly compatible heterogeneous nucleation cores for cementite. This insight offers a powerful theoretical basis and a practical, optimized process guideline—specifically, controlled SiC particle addition—for achieving high-strength and toughened as-cast ductile iron casting, opening a reliable pathway for advanced foundry applications.

← PREVIOUS
Current State and Automation Challenge...

NEXT →
Optimizing Robotic Grinding for Steel Ca...

Search...

Statement

Copyright & Permissions

Contact Us

Sending email to below, we will reply within 24 hours!

info@zhycasting.com

+86 18210515388(primary)

+86 010 53608660

From a specific inquiry or to schedule a foundry tour, we are always here on your disposal.

Credibility, Good Quality, Competitive Price ——

Order & Packing

Process Introduction

WHY CHOOSE ZHY?

Contact Us

Leading technology & Strong scientific working group.

Packing & Delivery

Engineer Strength
QC Procedure
Well-equipped Facilities

E: info@zhycasting.com
P: +86 18210515388
F: +86 010 53608660

Solar Kits
Luoyang Travel
China UAV
Electric Vehicle
AI Robots